Current-induced magnetization switching in exchange-biased spin valves for current-perpendicular-to-plane giant magnetoresistance heads

A. Deac,[1,3,*] K. J. Lee,[1,3] Y. Liu,[2] O. Redon,[1,3] M. Li,[2] P. Wang,[2] J. P. Nozières,[1] and B. Dieny[1]
[1]*SPINTEC, URA CEA/CNRS, CEA Grenoble/DRFMC, 17, Rue des Martyrs, 38054 Grenoble cedex 9, France*
[2]*Headway, 678 Hillview Drive, Milpitas, California 95035, USA*
[3]*CEA Grenoble/DRT/Leti, 17, Rue des Martyrs, 38054 Grenoble cedex 9, France*
(Received 1 December 2004; revised manuscript received 19 October 2005; published 9 February 2006)

In contrast to earlier studies performed on simple Co/Cu/Co sandwiches, we have investigated spin-transfer effects in complex spin-valve pillars with a diameter of 130 nm developed for current-perpendicular-to-plane magnetoresistive heads. The structure of the samples included an exchange-biased synthetic pinned layer and a free layer, both laminated by insertion of several ultrathin Cu layers. Despite the small thickness of the polarizing layer, our results show that the free layer can be switched between the parallel (P) and the antiparallel (AP) states by applying current densities of the order of 10^7 A/cm^2. A strong asymmetry is observed between the two critical currents $I_c^{\text{AP-P}}$ and $I_c^{\text{P-AP}}$, as predicted by the model of Slonczewski. Due to the use of exchange-biased structures, the stability phase diagrams could be obtained in the four quadrants of the (H,I) plan. The critical lines derived from the magnetoresistance curves measured with different sense currents, and from the resistance versus current curves measured for different applied fields, match each other very well. The main features of the phase diagrams can be reproduced by investigating the stability of the solutions of the Landau-Lifshitz-Gilbert equation including a spin-torque term, within a macrospin model.

DOI: 10.1103/PhysRevB.73.064414 PACS number(s): 85.75.−d, 72.25.Pn, 75.47.De, 75.70.−i

I. INTRODUCTION

It was predicted[1,2] that a spin-polarized electrical current flowing through a magnetic layer can exert a large torque on its magnetization, inducing magnetic excitations and eventually switching. The early experimental results demonstrating that it is indeed possible to switch the magnetization of a layer back and forth by applying an electric current[3] have attracted a considerable interest. Motivated by its potential application as an alternative write scheme in magnetic random access memories (MRAMs) or in magnetic recording technology, many efforts have been made ever since in order to understand the physics of this new phenomenon: new theoretical models[4–6] have been published, as well as numerical simulations[7–10] and experimental results.[11–16] At an earlier stage, the effect was studied only in very simple structures of the type *magnetic thick layer/nonmagnetic spacer/magnetic thin layer*, where the two magnetic layers were either CoFe or NiFe. Lately, however, more complicated structures were investigated, including current-perpendicular-to-plane (CPP) spin valves with pinned synthetic layers[17–19] and even magnetic tunnel junctions[20] (MTJs). More interest in this field has been stimulated by recent experiments showing that a spin-polarized current can drive the magnetization of a layer into steady precessional modes inaccessible by applying only a magnetic field.[21,22] These effects can be applied in new magnetic devices, such as resonators or microwave sources.

On the other hand, nowadays, the trend in high-density magnetic recording technology is to replace the current-in-plane (CIP) geometry in magnetoresistive heads for computer disk drives by the CPP configuration, since the latter offers larger magnetoresistance (MR) ratios and allows for higher storage density by reducing the shield-to-shield spacing. The required current densities are between 10^7 A/cm^2 and 10^8 A/cm^2, of the same order of magnitude as the currents at which spin-torque-induced magnetic excitations are observed. Such effects can generate noise and influence the biasing of the magnetic heads; therefore, it is important to study and understand them in order to control their influence.

II. SAMPLE PREPARATION AND EXPERIMENTAL SETUP

The present experiments were conducted on sputtered spin valves with the following structure: IrMn 7/AP2 4.0/Ru 0.8/AP1 4.4/Cu 2.6/F 3.6/Ta. All thicknesses are given in nm (see Fig. 1). The bottom electrode is a 1-μm-thick NiFe stripe, with its longer dimension (12 μm) along the pinning direction of the pinned layer; the top electrode is patterned from a Cu layer. The NiFe stripe is meant to constitute one of the magnetic shields in the real device. AP1 (polarizing) and F (free) are CoFe layers, laminated by the

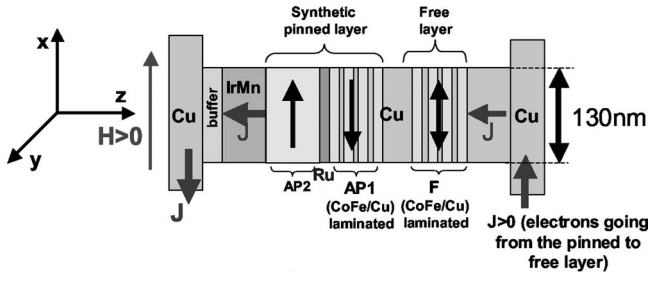

FIG. 1. The structure of the samples includes a laminated CoFe free layer and a laminated synthetic pinned layer. The pillars have a "square" section with a lateral size of 130 nm. The magnetization of the AP1 (polarizing) layer is oriented along the $-\mathbf{u}_x$ direction; the current is flowing along the $\mathbf{u}_z$ direction.

insertion of three ultrathin (0.3 nm) Cu layers. The purpose of the lamination is to increase the resistance of the part of the spin valve which is active from the point of view of the CPP giant magnetoresistance (GMR), i.e., the AP1/Cu/F sandwich. Indeed, at the lowest order of approximation, this active part can be considered as connected in series with the other layers, which are important to ensure suitable magnetic properties for read head applications, but reduce the CPP-GMR ratio because of their additional serial resistance. The increase in resistance due to lamination is significant, since each CoFe/Cu interface has a resistance equivalent to about 4 nm of bulk CoFe layer.[23] An enhancement from 1.5% to 2.2% of the CPP-GMR was observed in these structures due to the lamination.[24] However, this resulting increase in CPP-GMR amplitude is lower than expected from the relative increase of resistance because of significant spin flip at each CoFe/Cu interface. Indeed, it was shown[25] that the conduction electrons lose about 25% of their polarization at each Co/Cu interface. The same order of magnitude of depolarization may be expected at $Co_{50}Fe_{50}$/Cu interface. As a consequence, the electrons are almost fully repolarized along the direction of the local magnetization after having traversed less than 2 nm of the laminated stacks. This quite short effective spin-diffusion length in the laminated layers is responsible for the moderate benefit of lamination.

After the patterning of the bottom lead, electron-beam lithography and ion-beam etching were used to fabricate square pillars (with rounded corners) with a lateral size of 130 nm. An insulator layer (alumina) was then deposited. The top contacts were opened through a lift-off process. The last steps were the sputtering and the patterning of the top Cu lead, perpendicular to the bottom one. The layout allowed for four-probe point measurements, with two contacts placed on the top Cu lead and two on the bottom NiFe lead.

A simple setup was used for the experiments. External magnetic fields up to ±600 Oe could be applied using a small electromagnet, and a Keithley 2400 source meter was used both as a current source and as a voltmeter. Although quite reliable as a current source, the Keithley 2400 is less accurate as a voltmeter, which explains why sometimes a slight divergence was observed in the resistance versus current $[R(I)]$ curves around $I=0$. The resistance of the samples ranged between 5.6 and 8.8 Ω and the magnetoresistance amplitude was around 2.2%. The coercivity of the free layer ranged between 10 and 150 Oe, i.e., our soft layer was much softer than the thin layers used in all previous experiments reported in the literature. The dispersion from sample to sample is probably due to small differences in the detailed shape of the pillars, especially at their edges. A shift of a few tens of Oe was measured at low current in most samples in the position of the minor hysteresis loop associated with the switching of the free layer. This shift is due to the magnetostatic stray field from the pinned layer. As a result, in zero applied magnetic field, the samples were in the antiparallel state. This means that the stray field corresponds to a dominant interaction with the AP1 layer, which is closer to the free layer and slightly thicker than the AP2 layer.

Alternatively, magnetoresistance curves could be measured using a KLA Tencor tester with a maximum available field of ±1200 Oe. In most of the samples, the magnetization of the pinned layer started to switch around 1000 Oe, meaning that in the range ±600 Oe it remained unaffected. The KLA Tencor tester offers also the possibility of measuring the MR properties at temperatures ranging from room temperature (25 °C) to 110 °C. This option was used in order to determine the thermal variation of the resistance in the two magnetic configurations [parallel (P) and antiparallel (AP)] (Fig. 5).

All the other experiments were conducted at room temperature.

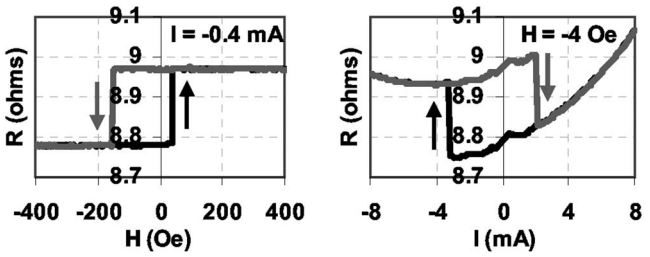

FIG. 2. (a) Magnetoresistance curve measured with a sense current $I=-0.4$ mA; the black curve is measured for increasing fields, the gray one for decreasing fields. Negative fields are oriented along the magnetization of the pinned layer (favor the P state). (b) Resistance versus current characteristics for $H=-4$ Oe. The gray (black) curve is measured for increasing (decreasing) currents. For the positive current, the electrons flow from the pinned to the free layer (see Fig. 1), thus favoring the P alignment.

III. RESULTS

In the discussion of the results, we use the following conventions (Fig. 1): (1) Negative magnetic field is oriented along the magnetization of the pinned AP1 layer; therefore, it favors the parallel alignment of the magnetizations of the two layers. (It follows that positive field favors the antiparallel orientation.) (2) For negative current, the electrons flow from the free to the pinned layer, favoring the antiparallel state. (Inversely, for positive current, the electrons move in the opposite direction and favor the parallel state.) Considering the size of our samples, an applied current of 1 mA corresponds to a current density of 0.59×10^7 A/cm^2.

Figure 2(a) shows a minor MR loop measured with a sense current of −0.4 mA. At such current density (-2.36×10^6 A/cm^2), we do not expect any spin-transfer-induced effects. The coercivity of this sample is $H_c=91$ Oe. The magnetostatic field from the synthetic pinned layer shifts the loop toward negative fields (i.e., the magnetostatic stray field is positive: $H_{ms}=48$ Oe), thus favoring the AP state. The low resistance state, $R_{min}=8.78$ Ω, corresponds to the P alignment, and the high resistance state, $R_{max}=8.97$ Ω, to the AP configuration. The MR amplitude is 2.16%. The same relative resistance variation is found between the two resistance levels on the $R(I)$ curve in Fig. 2(b); the values of the resistance in the two states are also very close to the ones measured in the $R(H)$ loop ($R_{min}=8.79$ Ω and $R_{max}=8.99$ Ω). We can therefore conclude that we have observed current-induced magnetization switching of the magnetization of the

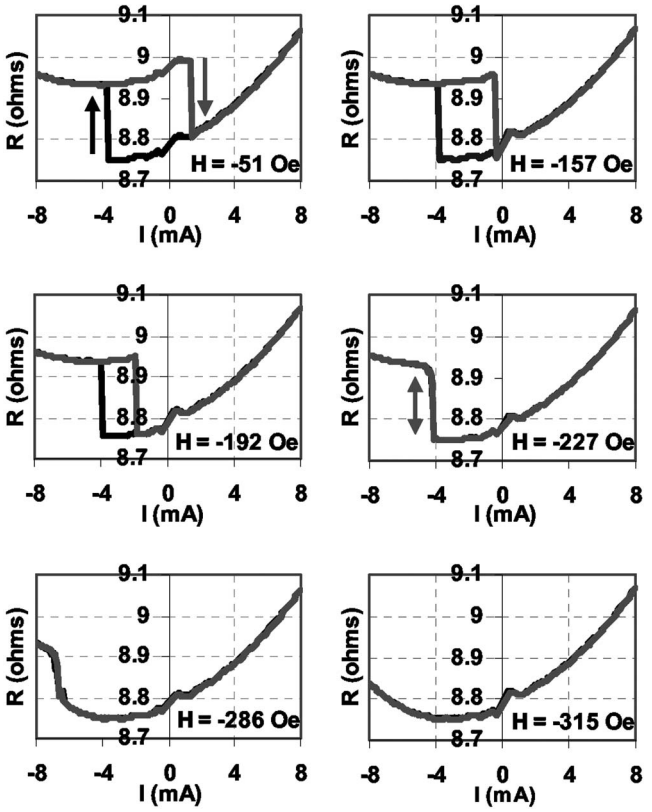

FIG. 3. Resistance versus current characteristics for increasing values of the negative applied field.

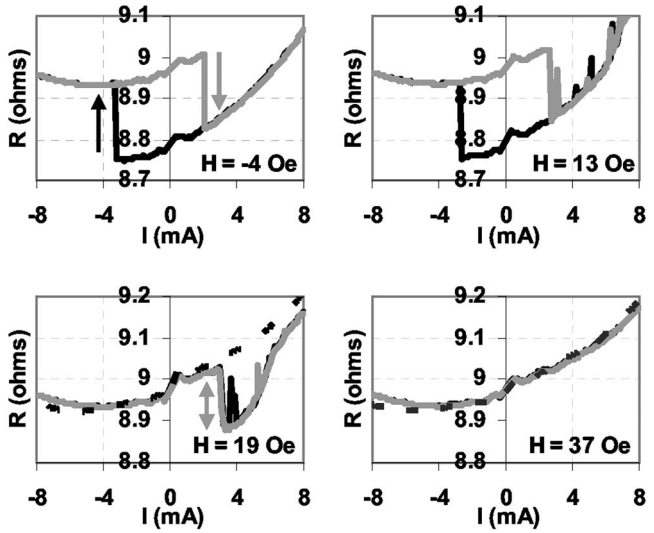

FIG. 4. Resistance versus current characteristics for increasing values of the positive applied field. The dotted curve ($H=19,37$ Oe) is measured at 600 Oe, when the sample should be in the AP state.

free layer between P and AP configurations. Starting with the sample in the AP state, a positive current $I_c^{\text{AP-P}}=2$ mA ($j_c^{\text{AP-P}}=1.18\times10^7$ A/cm^2) is needed in order to switch to the P state. Increasing the current even more leads to the heating of the sample, as indicated by the parabolic increase in the sample resistance. When sweeping the current backward, toward negative values, a P-AP transition occurs for $I_c^{\text{P-AP}}=-3.3$ mA ($j_c^{\text{P-AP}}=1.95\times10^7$ A/cm^2), after which the sample remains in the AP state until a (high enough) positive current is applied. This is in agreement with our convention regarding the sign of the current. The order of magnitude of the critical currents is the same as the other values so far reported in the literature. Both for the magnetoresistance and for the resistance versus current curves, the transitions between the two states are very sharp, indicating that sample is switching between two single-domain states.

In order to compare the $R(I)$ and $R(H)$ data, we have constructed the phase diagram characterizing the magnetic stability of the system in two different ways: For the same samples, we have measured the $R(I)$ curves for different applied fields and the magnetoresistance loops $R(H)$ for different sense currents.

Figure 3 shows the evolution of the resistance versus current characteristics while increasing the applied negative magnetic field. Considering the conventions for positive fields (which favor the P state), and for the sign of the current (positive current favors the P alignment), as long as the external field is not large enough, the AP-P transition occurs in negative currents, and the P-AP transition is induced by positive currents, as expected. At −51 Oe, when the magnetostatic field from the pinned layer is approximately compensated by the external field, a strong asymmetry is observed between the two switching currents, as predicted by Slonczewski's ballistic model (1996).[2] Increasing the external field induces a shift of the loop toward more negative currents. The AP-P transition shifts slowly at low fields (between 0 and approximately −140 Oe) and faster at larger fields. Simultaneously, the coercivity is gradually reduced, the AP-P transition being shifted more than the P-AP. At −227 Oe, the curve is practically reversible. At −315 Oe, the maximum applied current is no longer sufficient for inducing a P-AP transition, and the sample remains close to the P state (under the influence of the applied field).

The behavior of the sample in positive applied fields is unusual (Fig. 4). The curves present random noise in the current interval where the magnetization of the free layer should be oriented parallel to that of the reference layer. This noise diminishes when increasing the field, but, at the same time, a gradual reversible transition toward a higher resistance state appears for high values of the current. This reversible transition is moving toward lower values of the current when the field is increased. Simultaneously, the AP-P transition induced by the spin transfer is moving toward higher values of the current. For $H>37$ Oe, the sample remains in (or close to) the AP state and no switching is observed. The gray curve is measured at 600 Oe, when the sample is expected to be in the AP state.

Both Fig. 3 and Fig. 4 show raw data. The resistance change due to heating has not been subtracted, and it is highly asymmetric for the two directions of the current. This is a consequence of the different compositions of the top and the bottom electrode (Cu and NiFe, respectively), known as the Peltier effect. When a voltage is applied on the junction between two metals, it induces a temperature gradient between the two leads. The sign of the temperature gradient

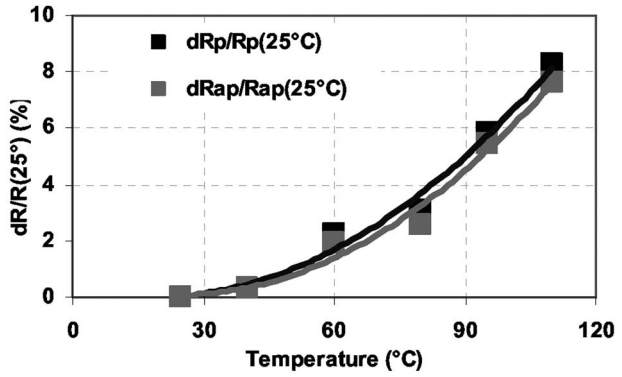

FIG. 5. Temperature variation of R^{AP} and R^{P} normalized to the respective values at room temperature, measured for a second sample with an identical structure.

depends on the sign of the voltage. In our case, for a positive voltage, the hot electrode is the Cu-pillar system; for a negative voltage, the hot electrode is the NiFe lead. The measured resistance variation is due to the combination of the Joule heating ($\sim I^2$) and the Peltier heating or cooling ($\sim I$). In order to estimate the variation in temperature due to the combination of Joule and Peltier effects, we have measured the thermal variation of the resistance of the sample in the range 25–110 °C (see Fig. 5). Figure 2(b) shows that increasing the current from 0.4 mA to 8 mA yields a resistance increase of 2.95%. The comparison with Fig. 5 indicates that this corresponds to a raise in temperature of about 50 °C at 8 mA. For negative current, a decrease of resistance of about 0.5% is first observed from −0.4 mA to −5 mA (the Peltier cooling dominating the Joule heating) followed by an increase of 0.5% between −4 mA and −8 mA (the Joule heating dominating the Peltier cooling) [Fig. 2(b)]. According to Fig. 5, this corresponds to a decrease then increase of temperature of less than 10 °C. We underline that these estimations of temperature variations are averaged over the entire pillar. Locally, the temperature variation can be larger. This interpretation in terms of Joule and Peltier effects is supported by the observation that samples having two identical leads do not show any heating dependence on the polarity of the current.

An alternative procedure for studying spin-transfer-induced effects consists in measuring magnetoresistance curves for different applied currents (Figs. 6 and 7). Increasing the negative sense current (Fig. 6) up to −3 mA induces a slight shift of the loop toward positive fields; this observation is in good agreement with the fact that for negative currents the spin-transfer torque tends to stabilize the AP state, since the electrons are flowing from the free layer to the pinned layer. The coercivity is not much affected in this range of current. Between −3 mA and −4 mA, the P-AP transition jumps from ~0 Oe to ~200 Oe, and the coercivity is virtually zero. This is probably because at this value, the current density is large enough to induce the P-AP transition of the free layer. The AP-P transitions still occur under the influence of the applied magnetic field. Increasing the current over −4 mA causes a faster shift of the loop and probably the formation of a vortex distortion. The transition between the two states becomes more and more slanted. In addition, the

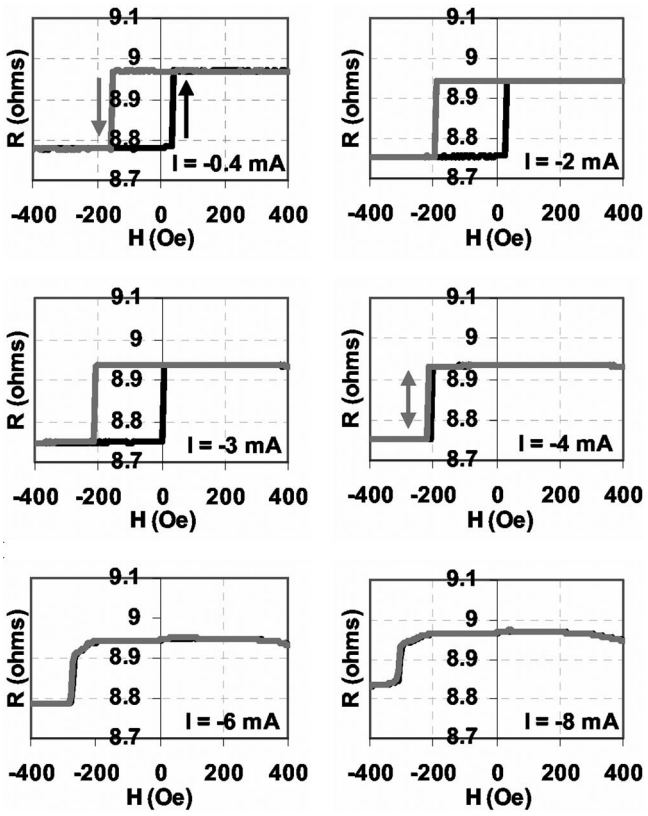

FIG. 6. Magnetoresistance curves for increasing values of the negative sense current.

magnetoresistance amplitude drops from 2.16% for $I=-0.4$ mA to less than 1.5% at ±7.5 mA. When applying a positive sense current (Fig. 7) up to 2 mA, the transition AP-P is shifting toward more positive values, while the P-AP transition remains practically unchanged. At $I=2$ mA, the switching becomes reversible. Further increasing the current only yields a more pronounced slanting of the transition, but no additional shift is measured.

A remarkably good agreement is obtained when superposing on the same plot the critical lines deduced from the resistance versus current curves for constant applied (negative) magnetic fields and from the magnetoresistance curves measured with different (negative and positive) sense currents (Fig. 8). Following the approach of Grollier *et al.*,[27] we have plotted the switching currents ($I_c^{AP\text{-}P}$ and $I_c^{P\text{-}AP}$) or the switching fields ($H^{AP\text{-}P}$ and $H^{P\text{-}AP}$) if the loop was hysteretic, and the beginning and the end of the transitions (I^{start} and I^{end} or H^{start} and H^{end}), if they were reversible. Four distinct regions are identified: (1) Both the P and the AP states are stable in between the $I_c^{AP\text{-}P}$ and $I_c^{P\text{-}AP}$, respectively, $H^{AP\text{-}P}$ and $H^{P\text{-}AP}$, curves. (2) Only the P state is stable above the $I_c^{AP\text{-}P}$ ($H^{AP\text{-}P}$) and I^{start} (H^{start}) lines. (3) Only the AP state is stable under the $I_c^{P\text{-}AP}$ ($H^{P\text{-}AP}$) and I^{end} (H^{end}) lines: (4) Neither state is stable between the I^{start} and I^{end}, respectively, H^{start} and H^{end}, curves. Both series of measurements [$R(I)$ for different H and $R(H)$ for different I] have been repeated, yielding similar results.

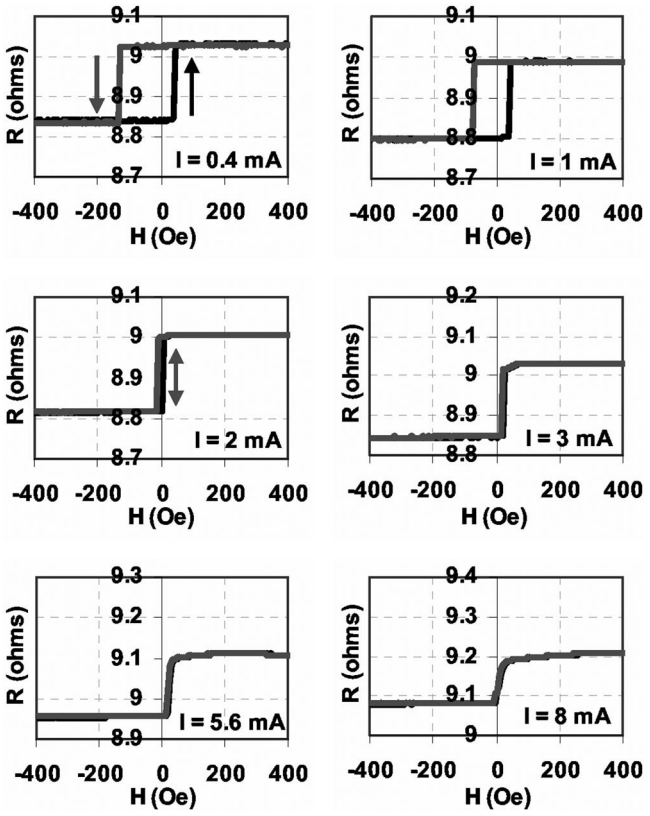

FIG. 7. Magnetoresistance curves for increasing values of the positive sense current.

IV. DISCUSSION

Following the macrospin approach of the spin-torque-induced dynamics,[26,27] and taking into account our conventions for the sign of field and current, the Landau-Lifshitz-Gilbert equation of motion of the free layer's magnetization can be written as follows:

$$\frac{\partial \vec{m}}{\partial t} = -\gamma\, \vec{m} \times [H_{res}\vec{u}_x - H_d(\vec{m}\cdot\vec{u}_z)\cdot\vec{u}_z] + \alpha\, \vec{m}\frac{\partial \vec{m}}{\partial t} - \frac{\hbar}{2e}\frac{\gamma}{M_s A t} g(\theta) I\, \vec{m} \times [\vec{m} \times (-\vec{u}_x)], \quad (1)$$

where $\vec{m}$ is the unit vector of the magnetization of the free layer; $\gamma_0 = 1.76 \times 10^{-11}$ s^{-1} T^{-1} is the gyromagnetic ratio; $H_{res} = H + H_{ms} \mp H_c$ is the total field on the free layer, when its magnetization is close to the P (−) or AP (+) state; H is the external applied magnetic field, H_{ms} the magnetostatic field from the pinned layer, and H_c the coercivity of the free layer; $H_d = 4\pi M_s$ is the demagnetizing field; α is the damping constant; I is the applied current; t the thickness, A the area of the free layer (in our case, $t = 3.6$ nm); $e = 1.6 \times 10^{-19}$ C is the electron charge; $\hbar$=Plank's constant; $g(\theta)$ is a function which describes the angular dependence of the spin torque (θ being the angle between the magnetization of the two layers); $\vec{u}_x$ is the unit vector parallel to the magnetization of the free (and pinned) layer, $\vec{u}_z$ is the unit vector perpendicular to the plane of the layers (along the direction of the current) (see Fig. 1 for the definition of the coordinate system).

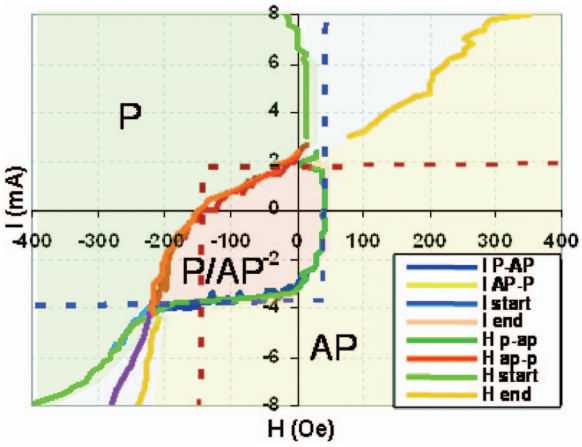

FIG. 8. (Color) The phase diagram obtained from the resistance versus current curves for constant applied (negative) magnetic fields, and from the magnetoresistance curves measured with different (negative and positive) sense currents. We have plotted the switching currents ($I_c^{\text{AP-P}}$ and $I_c^{\text{P-AP}}$) or the switching fields ($H^{\text{AP-P}}$ and $H^{\text{P-AP}}$) if the loop was hysteretic, and the beginning and the end of the transitions (I^{start} and I^{end} or H^{start} and H^{end}), if they were reversible. The dotted lines represent the theoretical fit.

The first term in Eq. (1) is the field-induced precession term; the second one is the Gilbert damping; and the third is the contribution of the spin torque. The spin torque can act as damping or antidamping, depending on the relative effects of the total field and the applied current.[7] Note that in our coordinate system, the magnetization of the pinned layer is parallel to $-\vec{u}_x$ (negative field favors the P alignment).

We solved Eq. (1) following the method of Grollier *et al.*[27] After projection of Eq. (1) on the x, y, z axes, and considering that the magnetization of the free layer is close to either the P or the AP state ($m_x = \mp 1, \dot{m}_x = 0$), the following stability conditions can be deduced for the two orientations of the free layer relative to the pinned layer. (1) the P state is unstable when

$$I < \frac{2e}{\hbar}\frac{\alpha M_s A t}{g(0)}\left(-\frac{H_d}{2} + H_{ms} - H_k + H\right), \quad \text{if } H < -H_{ms} + H_c,$$

$$I < \frac{2e}{\hbar}\frac{\alpha M_s A t}{g(0)}\left(-\frac{H_d}{2} + H_{ms} - H_k + H\right) + \frac{2e}{\hbar}\frac{M_s A t}{g(0)}\sqrt{(H_{ms} - H_k + H)(H_d - H_{ms} + H_k - H)}, \quad \text{if } H < -H_{ms} + H_c, \quad (2)$$

(2) The AP state becomes unstable for

$$I > \frac{2e}{\hbar}\frac{\alpha M_s A t}{g(\pi)}\left(\frac{H_d}{2} + H_{ms} + H_k + H\right) - \frac{2e}{\hbar}\frac{M_s A t}{g(\pi)}\sqrt{-(H_{ms} + H_k + H)(H_d + H_{ms} + H_k + H)}, \quad \text{if } H < -H_{ms} - H_c,$$

$$I > \frac{2e}{\hbar}\frac{\alpha M_s A t}{g(\pi)}\left(\frac{H_d}{2} + H_{ms} + H_k + H\right), \quad \text{if } H < -H_{ms} - H_c. \tag{3}$$

In order to fit the experimental phase diagram, we have used these formulas to determine the critical lines characterizing the currents at which magnetic switching is observed (Fig. 8). A reasonably good agreement with the experimental data was obtained for the following parameters: $H_c=91$ Oe, $H_{ms}=48$ Oe, $H_d=16\,000$ Oe, $\alpha=0.01$, $g(0)=0.246$, and $g(\pi)=0.526$. $g(0)$ and $g(\pi)$ were taken as fitting parameters, but the values we found are quite close to those calculated by Stiles and Zangwill[28] for Co/Cu/Co trilayers, and could be used to fit phase diagrams for several samples. The values considered for H_d and α are typical for such structures.

As predicted by Slonczewski's ballistic model (1996),[2] there is a strong asymmetry ($I_c^{\text{AP-P}} > I_c^{\text{P-AP}}$) for $H=-51$ Oe (when the applied field compensates the magnetostatic interaction from the pinned layer). However, when using Slonczewski's formula for $g(\theta)$ as a function of the polarization of the current, one would expect a much higher $I_c^{\text{AP-P}}/I_c^{\text{P-AP}}$ ratio than the one we measured.

Above the blue dotted line, the P state is stable; the AP state is stable under the brown dotted line. Consequently, five regions can be distinguished: one region where both states are stable (the coercivity region, in the center of the diagram), one region were only the P state is stable, one region were only the AP state is stable, and two regions where neither state is stable (high positive and/or negative fields). In the macrospin model,[27] these latter regimes are attributed to steady precession motions of the free layer's magnetization. Such states have been recently demonstrated experimentally.[21]

This simple macrospin model can be used to fit several features of the experimental phase diagram: (1) the general shape of the phase diagram, as well as the existence of four types of regions (P stable, AP stable, both P and AP stable and both P and AP unstable, i.e., precession region); (2) the values of the applied field for which the border lines change from a linear dependence to a parabolic one ($H=43$ Oe for P, $H=-139$ Oe for AP stable), as well as the linear dependence of the instability current for P when $H<43$ Oe and for AP when $H>-139$ Oe, and the parabolic (-like) dependence elsewhere; (3) the values of $I_c^{\text{AP-P}}$ and $I_c^{\text{P-AP}}$ for $H=0$ Oe; (4) the slope of $I_c^{\text{P-AP}}$ as a function of H for -210 Oe$<H<43$ Oe. Other features of the experimental phase diagram cannot be explained, such as (1) the slope of $I_c^{\text{AP-P}}$ as a function of H for $H>-139$ Oe; (2) the curvature of I^{end} for $H<-139$ Oe; (3) the linear dependence of the instability current for P, when $H<-200$ Oe.

The disagreements between the theoretical and the experimental limits of the steady precession region can be at least partially explained by the fact that the model does not consider the influence of the Oersted field generated by the current. This field can be quite important in this region (about 150 Oe for an applied current of 4 mA), favoring the formation of a vortex distortion, not taken into consideration by the macrospin model. Several micromagnetic studies have underlined the importance of the Oersted field in the investigation of current-induced magnetization switching.[9,29] It was even suggested that in Co/Cu/Co circular nanopillars with a diameter of 130 nm (similar to our samples), the field induced by the current plays a crucial role in promoting the switching.[29] Even for samples with important shape anisotropy, several features of the phase diagrams cannot be explained without taking into account the Oersted field.[9]

The formation of a vortex distortion in the free layer when increasing the applied (positive and negative) current also yields a decrease in the magnetoresistance amplitude. However, other effects intrinsic to the spin transfer could also contribute. First, under certain conditions, the spin-polarized current can induce GHz precession states of the magnetization of the free layer along out-of-plane orbits.[9,10,21,22] Second, different micromagnetic[9] and experimental[12,30] studies have shown that spin transfer can cause telegraph noise either between the P and AP states (inside the coercivity region) or between almost P and AP states corresponding to different precession orbits, even at 0 K. The dwell time of such telegraph noise is much shorter (of the order of nanoseconds) than the characteristic time of our experiment (several milliseconds), which means the resistance we measure is statically averaged over this interval. The decrease of the magnetoresistance in high currents is probably the conjoint consequence of all these phenomena, and only high-resolution time-resolved and frequency-dependent measurements could shade more light on this point.

The theoretical critical lines on the phase diagram are calculated at $T=0$ K. It has been shown that thermal effects reduce the critical currents and the switching fields in the coercivity region and cause a rounding of the phase diagram and an increase of the slope of the critical lines in the coercivity region.[31] It is difficult to treat the thermal effects quantitatively for two different reasons: First, for positive currents the temperature of the sample increases very rapidly with the current, while for negative currents the temperature of the sample is approximately constant; second, an Arrhenius-type treatment would not necessarily be appropriate in this case, since the dwell time of the telegraph noise caused by the spin transfer is of the order of the attempt time used in the Arrhenius law of thermal activation ($\tau_0 \sim 1$ ns).

From a general comparison of our phase diagram with the theory, we observe that the macrospin model fits the P-AP transition (which occurs mostly for negative currents) better than the AP-P one (observe most of the times for positive currents). Such behavior has been observed earlier in simpler structures. In our samples, the agreement between theory and experiment is expected to be better at negative currents, which are less affected by heating effects.

The effect of the finite temperature on the switching fields is taken into account by using the measured room temperature coercivity of the sample instead of the 0 K anisotropy field in the formulas for the critical lines; as a consequence, we find that the experimental critical lines and the theoretical fits change slopes for the same values of the field.

It is important to note that within this simple model, it is only possible to calculate the values of the current where a given state becomes unstable. As it was often commented in the literature, it does not necessarily follow that the free layer actually switches to the opposite orientation. Furthermore, as

it was mentioned previously,[26] it is somewhat difficult to identify the exact beginning and end of the reversible transitions on the curves, which could also result in discrepancies between experiment and theory. Moreover, it has been shown that the macrospin model is a poor approximation for describing the magnetic dynamics of the free layer during the current-induced magnetization switching. Indeed, the dynamics is most often very chaotic during before and during the reversal.[9] Nevertheless, the simple theory described above offers a satisfactory semiquantitative comprehension of the general features of the *I-H* phase diagram.

The macrospin model also fails to explain the presence of the gradual transition toward the AP state at positive current, in the (small) positive applied field range, as well as the random noise measured under the same conditions. Indeed, in our configuration, positive current favors the parallel alignment between the magnetizations of the two layers, and the AP-P transition induced by spin transfer occurs for small positive values of the current. Increasing the current should furthermore stabilize the P state. For example, for an applied field of 19 Oe, both the magnetostatic field from the pinned layer and the external field favor the AP orientation of the two layers. Starting with the sample in the AP state, when sweeping the current from negative to positive values, the spin-transfer-induced transition occurs at $I_c^{\mathrm{AP\text{-}P}}=3.1$ mA. At this value, the spin-torque effect becomes stronger than that of the resultant field acting on the magnetization of the free layer. Since, for the positive current, the electrons flow from the pinned to the free layer, increasing the current should not change the state of the sample. However, at 5 mA, the free layer starts to relax back to a higher resistance state, as seen in Fig. 4. This second transition cannot be explained by the formation of a vortex induced by the Oersted field of the current, since the resistance at 8 mA is closer to the resistance of the AP state than to that in a vortex configuration.

It is indeed interesting to note that the system evolves to a static resistance level which is closer to that of the antiparallel state (favored by the field) than to that of the parallel configuration (favored by the current). Frequency-domain experiments[32] showed that in this area of the phase diagram, increasing the current leads to an increase of the precession angle, since the precession frequency is decreasing, and eventually to high-frequency telegraph noise. However, positive current favors the parallel orientation of the magnetization of the free layer with respect to the reference layer, and switching to the P state occurs for currents of the order of 2–3 mA. Consequently, an evolution of the system toward a higher resistance state for currents larger than the critical current (and an increase of the precession cone) can only be induced by an increasing positive field. Since no additional field is applied, other than the static external field specified on each $R(I)$ curve, the only other field that would justify such a behavior is the Oersted field. Indeed, without spin torque, the joint effect of the positive applied field, positive magnetostatic interaction from the reference layer (which is much stronger on the edges than in the center) and circular-symmetry Oersted field, the local moments of the free layer would arrange themselves into an off-centered vortex state, with a majority of moments pointing along the positive direction of the field. Since spin transfer favors the opposite orientation, these moments will precess along an orbit which depends on the current intensity and the local field. Increasing the current leads to an increased spin torque, but also an enhanced Oersted field. Under these conditions, it is possible that the precession cone increases with the applied current. Moreover, the high temperature reached locally for high positive currents furthermore destabilizes the P state. However, such effects, which are expected to be more obvious in ranges of current and field where the sample should be in the P state (destabilized by the magnetostatic interaction between layers and higher temperature for positive currents), cannot be taken into account within the frame of a simple macrospin model, but only through micromagnetic simulations.

Finally, as we have argued before,[19] we emphasize that we observed spin-transfer-induced effects in these samples, although the AP1 polarizing layer (4.4 nm) is much thinner than the hard magnetic layer in commonly used samples in which spin-transfer effects were investigated before. The thickness of the AP1 layer is even smaller than the spin-diffusion length in bulk $Co_{50}Fe_{50}(6\pm1$ nm).[24] Because of the lamination of the pinned layer, as discussed in the introduction, the effective spin-diffusion length in the laminated stack is reduced to 1.2 ± 0.1 nm due to increased interfacial scattering and higher density of thermally activated magnetic fluctuations.[24] Consequently, a significant current polarization can build up in this layer, which explains the large measured spin-transfer effects.

V. CONCLUSION

We have demonstrated that large spin-transfer-induced effects, in particular current-induced magnetization switching, can be observed in complex spin-valve structures developed for CPP magnetic heads. The macrospin model can reasonably well account for the experimental results. Overall, the general trends characterizing spin transfer in complex spin valves with SAF exchange-biased layer and laminated magnetic films are found to be consistent with the widely studied Co/Cu/Co nanopillars. The comparison holds mainly for negative fields, since, as mentioned several times before, in simple pseudospin valves with an unpinned reference layer, only the part of the phase diagram corresponding to fields applied parallel to the reference layer can be fully investigated.

ACKNOWLEDGMENTS

The authors would like to thank Professor A. Vedyaev, Professor N. Ryzhanova, Dr. N. Strelkov, and Dr. K. Ju for fruitful discussions, and Dr. U. Ebels and Dr. D. Stanescu for helping with the experimental setup. This work was partially supported by the IST project NEXT (IST-37334) and the RMNT project MAGMEM II.

*Electronic address: alina.deac@excite.com

[1] L. Berger, Phys. Rev. B **54**, 9353 (1996); **59**, 11465 (1999).
[2] J. Slonczewski, J. Magn. Magn. Mater. **159**, L1 (1996); **195**, L261 (1999).
[3] A. Katine, F. J. Albert, R. A. Buhrman, E. B. Myers, and D. C. Ralph, Phys. Rev. Lett. **84**, 3149 (2000).
[4] S. Zhang, P. M. Levy, and A. Fert, Phys. Rev. Lett. **88**, 236601 (2002).
[5] M. D. Stiles and A. Zangwill, Phys. Rev. B **66**, 014407 (2002).
[6] J. Z. Sun, Phys. Rev. B **62**, 570 (2000).
[7] Z. Li and S. Zhang, Phys. Rev. B **68**, 024404 (2003).
[8] Z. Li and S. Zhang, Phys. Rev. B **69**, 134416 (2004).
[9] K. J. Lee, A. Deac, O. Redon, J. P. Nozières, and B. Dieny, Nat. Mater. **3**, 877 (2004).
[10] J-G. Zhu and X. Zhu, IEEE Trans. Magn. **40**, 182 (2004).
[11] J. Grollier, V. Cros, A. Hamzic, J. M. George, H. Jaffres, A. Fert, G. Faini, J. Ben Youssef, and H. Legall, Appl. Phys. Lett. **78**, 3663 (2001).
[12] S. Urazhdin, H. Kurt, W. P. Pratt, Jr., and J. Bass, Appl. Phys. Lett. **83**, 114 (2003).
[13] E. B. Myers, F. J. Albert, J. C. Stankey, E. Bonet, R. A. Buhrman, and D. C. Ralph, Phys. Rev. Lett. **89**, 196801 (2002).
[14] F. J. Albert, N. C. Emley, E. B. Myers, D. C. Ralph, and R. A. Buhrman, Phys. Rev. Lett. **89**, 226802 (2002).
[15] J. Z. Sun, D. J. Monsma, M. J. Rooks, and R. H. Koch, Appl. Phys. Lett. **81**, 2202 (2002).
[16] B. Özyilmaz, A. D. Kent, D. Monsma, J. Z. Sun, M. J. Rooks, and R. H. Koch, Phys. Rev. Lett. **91**, 067203 (2003).
[17] M. Covington, A. Rebei, G. J. Parker, and M. A. Seigler, Appl. Phys. Lett. **84**, 3103 (2004).
[18] N. C. Emley, F. J. Albert, E. M. Ryan, I. N. Krivorotov, D. C. Ralph, and R. A. Buhrman, Appl. Phys. Lett. **84**, 4257 (2004).
[19] K. J. Lee, Y. Liu, A. Deac, M. Li, J. W. Chang, S. Liao, K. Ju, O. Redon, J. P. Nozières, and B. Dieny, J. Appl. Phys. **95**, 7423 (2004).
[20] Y. Huai, F. Albert, P. Nguyen, M. Pakala, and T. Valet, Appl. Phys. Lett. **84**, 3118 (2004).
[21] S. I. Kiselev, J. C. Sankey, I. N. Krivorotov, N. C. Emley, R. J. Schoelkopf, R. A. Buhrman, and D. C. Ralph, Nature (London) **425**, 380 (2003).
[22] M. Covington, M. Al Haj Darwish, Y. Ding, N. J. Gokemeijer, and M. A. Seigler, Phys. Rev. B **69**, 184406 (2004).
[23] W. Oepts, M. A. M. Gijs, A. Reinders, R. M. Jungblut, R. M. J. van Gansewinkel, and W. J. M. de Jonge, Phys. Rev. B **53**, 14024 (1996).
[24] M. Li, S. Liao, C. P. Chen, K. Ju, F. Delille, N. Strelkov, and B. Dieny (unpublished).
[25] K. Eid, W. P. Pratt, and J. Bass, J. Appl. Phys. **93**, 3445 (2003).
[26] A. Fert, V. Cros, J. M. George, J. Grollier, H. Jaffrès, A. Hamzic, A. Vaurès, G. Faini, J. Ben Youssef, and H. Le Gall, J. Magn. Magn. Mater. **272-276**, 1706 (2003).
[27] J. Grollier, V. Cros, H. Jaffrès, A. Hamzic, J. M. George, G. Faini, J. Ben Youssef, H. Le Gall, and A. Fert, Phys. Rev. B **67**, 174402 (2003).
[28] M. D. Stiles and A. Zangwill, J. Appl. Phys. **91**, 6812 (2002).
[29] L. Torres, L. Lopez-Diaz, E. Martinez, M. Carpentieri, and G. Finocchio, J. Magn. Magn. Mater. (to be published).
[30] J. E. Wegrowe, Phys. Rev. B **68**, 214414 (2003).
[31] M. A. Zimmler, B. Özyilmaz, W. Chen, A. D. Kent, J. Z. Sun, M. J. Rooks, and R. H. Koch, Phys. Rev. B **70**, 184438 (2004).
[32] A. Deac *et al.* (unpublished).